Molecular Therapy
Methods & Clinical Development
Original Article

High value of ^{64}Cu as a tool to evaluate the restoration of physiological copper excretion after gene therapy in Wilson's disease

Oihana Murillo,[1,7] Maria Collantes,[2,3,7] Cristina Gazquez,[1] Daniel Moreno,[1] Ruben Hernandez-Alcoceba,[1] Miren Barberia,[1] Margarita Ecay,[3] Blanche Tamarit,[4] Anne Douar,[4] Veronica Ferrer,[4] Jean Philippe Combal,[4] Ivan Peñuelas,[2,3] Bernard Bénichou,[4,6] and Gloria Gonzalez-Aseguinolaza[1,5,6]

[1]Gene Therapy and Regulation of Gene Expression Program, Centro de Investigacion Medica Aplicada (CIMA), FIMA, Navarra Institute for Health Research (IdisNA), University of Navarra, Avda Pio XII 55, 31008 Pamplona, Spain; [2]Department of Nuclear Medicine, IdisNA, Clinica Universidad de Navarra, 31008 Pamplona, Spain; [3]Translational Molecular Imaging Unit, IdisNA, Clinica Universidad de Navarra, 31008 Pamplona, Spain; [4]Vivet Therapeutics SAS, Paris, France; [5]Vivet Therapeutics S.L., Pamplona, Spain

Wilson's disease (WD) is an inherited disorder of copper metabolism associated with mutations in *ATP7B* gene. We have shown that the administration of an adeno-associated vector (AAV) encoding a mini version of human ATP7B (VTX-801) provides long-term correction of copper metabolism in a murine WD model. In preparation of a future clinical trial, we have evaluated by positron emission tomography (PET) the value of ^{64}Cu biodistribution, excretion pattern, and blood kinetics as pharmacodynamic biomarkers of VTX-801 effects. Six-week-old WD mice were injected intravenously with increasing doses of VTX-801 and 3 weeks or 3 months later with [^{64}Cu]$CuCl_2$. Untreated WD and wild-type (WT) mice were included as controls. Control WD mice showed increased hepatic ^{64}Cu retention, reduced fecal excretion of the radiotracer, and altered ^{64}Cu blood kinetics (BK) compared with WT mice. VTX-801 treatment in WD mice resulted in a significant reduction of hepatic ^{64}Cu accumulation, the restoration of fecal ^{64}Cu excretion, and the correction of ^{64}Cu BK. This study showed that VTX-801 restores physiological copper metabolism in WD mice, confirming the mechanism of action of VTX-801, and demonstrated the translational potential of [^{64}Cu]$CuCl_2$-PET to explore VTX-801 pharmacodynamics in a minimally invasive and sensitive manner in WD patients.

INTRODUCTION

Wilson's disease (WD) is a rare autosomal recessive, debilitating, and life-threatening disorder of copper homeostasis that affects approximately one in 30,000 individuals, with wide geographical variations.[1] In WD, mutations of the copper transporter ATP7B lead to decreased biliary copper excretion and a reduction in circulating holoceruloplasmin levels.[1–3] As a result, toxic levels of copper accumulate, primarily in the liver but also in the central nervous system; left untreated, WD is considered uniformly fatal. Current medical WD management includes copper chelators and/or zinc salt treatment, together with low-copper diet.[2–5] Despite recognized benefits, current life-long management options have important limitations, including poor compliance, incomplete resolution of symptoms, and various side effects, among them severe and often not fully reversible neurological deterioration.[2,3] As of today, liver transplantation, together with life-long immunosuppression, remains the only therapeutic option that can permanently restore physiological copper metabolism and is mostly limited to patients with acute liver failure or end-stage liver disease.[2–5] However, recent data suggest the potential for added benefit of liver transplantation to newly diagnosed neurological WD patients unresponsive to medical treatment.[6]

Liver-directed adeno-associated vector (AAV)-based gene therapy has been recently shown to offer a non-surgical, permanent correction of copper metabolism in WD mice.[7–9] The administration of VTX-801, a hepatotropic recombinant AAV carrying an *ATP7B*-minigene under the transcriptional control of a liver-specific promoter, to WD mice resulted in the reduction of copper concentration in liver and urine, restoration of fecal copper excretion, and normalization of ceruloplasmin activity and transaminase levels in circulation.[8,9] Furthermore, sustained therapeutic efficacy was demonstrated for at least 1 year with preserved liver histology and increased animal survival.[8]

In anticipation of a first-in-human clinical trial, we have explored the possibility of using a non-invasive technique to demonstrate the restoration of physiological copper metabolism in VTX-801-treated patients. Pioneering studies performed in the 50s–60s showed

Received 10 November 2021; accepted 3 June 2022;
https://doi.org/10.1016/j.omtm.2022.06.001.

[6]Senior author

[7]These authors contributed equally

Correspondence: Gloria Gonzalez-Aseguinolaza, Gene Therapy and Regulation of Gene Expression Program, Centro de Investigacion Medica Aplicada (CIMA), FIMA, Navarra Institute for Health Research (IdisNA), University of Navarra, Avda Pio XII 55, 31008 Pamplona, Spain.
E-mail: ggasegui@unav.es; ggonzalez@vivet-therapeutics.com

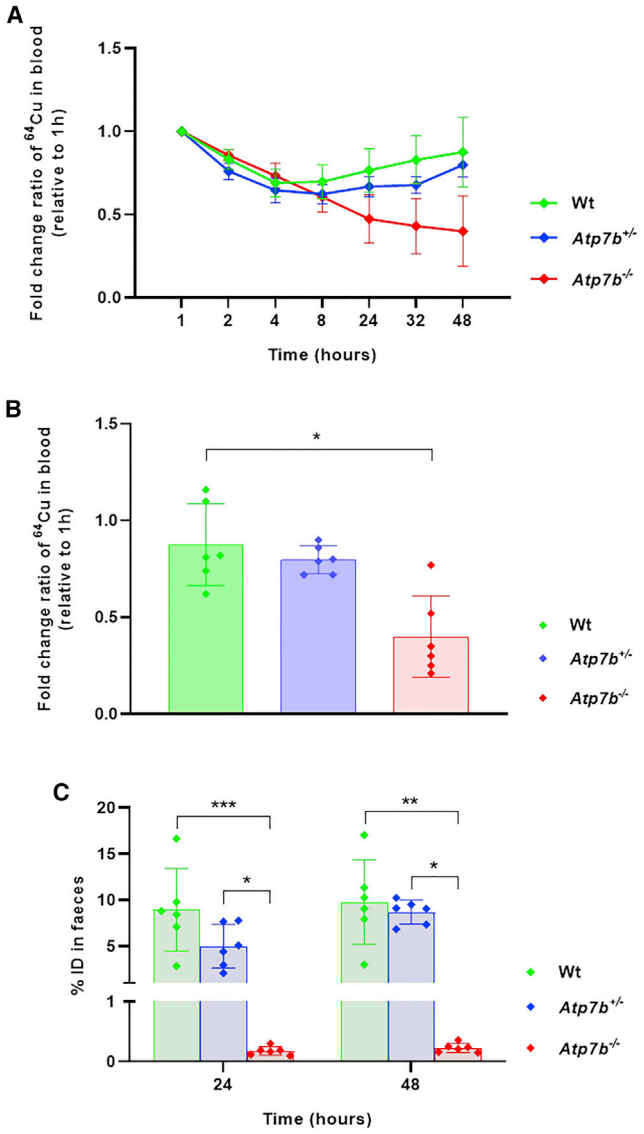

Figure 1. ^{64}Cu kinetics in blood and feces of WT, *Atp7b*$^{+/-}$, and *Atp7b*$^{-/-}$ mice at 9 weeks of age

Blood samples were collected 1, 2, 4, 8, 24, 32, and 48 h post-^{64}Cu administration. Feces were harvested 24 and 48 h after ^{64}Cu administration. (A) Radiocopper blood kinetics (BK) and fold change ratios of ^{64}Cu in blood relative to 1 h are shown. (B) Forty-eight-hours-to-one-hour ratio of ^{64}Cu in the serum is shown. (C) Cumulative fecal excretion of ^{64}Cu is shown. All data were presented as mean ± standard deviation (SD). The statistical analysis was performed using the non-parametric Kruskal-Wallis test followed by Dunn's multiple comparison post hoc. *p < 0.05; **p < 0.01; ***p < 0.001.

abnormal copper metabolism (reduced fecal excretion and abnormal plasma kinetics) in WD patients using radioactive copper isotopes, including short-lived ^{64}Cu.[10–12] The excellent WD diagnostic accuracy of the 48-h-to-1-to-2-h ^{64}Cu plasma ratio following intravenous [^{64}Cu]$CuCl_2$ administration showed initially by Sternlieb and Scheinberg[13] was recently corroborated by Czlonkowska et al.[14]

Here, we have investigated the biodistribution and excretion and secretion pattern of Cu after VTX-801 treatment in a murine model of WD using ^{64}Cu. Its use makes possible to perform non-invasive *in vivo* imaging studies for assessment of copper metabolism imbalance with positron emission tomography (PET) technology. In addition, the presence of ^{64}Cu in biological samples and tissues was measured in a gamma counter, adding valuable information about copper biodistribution and routes of elimination.

RESULTS

Distinctive biodistribution pattern of radiocopper in 9-week-old Atp7b$^{-/-}$ and WT mice

To set up optimal experimental conditions for the evaluation of VTX-801's effect on copper metabolism, we first studied the biodistribution of copper-64 in untreated 9-week-old *Atp7b*$^{-/-}$ (WD), *Atp7b*$^{+/-}$ (heterozygous), and WT (*Atp7b*$^{+/+}$) male (n = 3) and female (n = 3) mice (total n = 6). Blood samples were harvested at different time points, weighted, and measured in gamma counter. All animal groups showed a rapid decrease of the radioactive signal in blood shortly after injection, followed by a slight signal increase (starting 8 h post-injection) in WT and *Atp7b*$^{+/-}$ animals, and a distinctive continuous decrease in *Atp7b*$^{-/-}$ mice (Figure 1A). The average 48-h-to-1-h ratio of radiocopper signal in blood was 0.87 for WT animals, 0.79 for *Atp7b*$^{+/-}$, and 0.4 for *Atp7b*$^{-/-}$, being similar for WT and *Atp7b*$^{+/-}$, although statistically different between *Atp7b*$^{-/-}$ versus WT (Figure 1B). These data are consistent with data reported in humans.[13] During the experiment, all animals were placed in individual metabolic cages. Twenty-four-hour cumulative feces and urine were harvested for 2 consecutive days, and the presence of radioactive signal was determined (Figure 1C). Significant differences in the concentration of copper-64 in feces were observed between *Atp7b*$^{-/-}$ and WT or *Atp7b*$^{+/-}$ mice. While fecal excretion of radiocopper was observed in WT and Atp7b$^{+/-}$ mice, the signal was nearly undetectable in *Atp7b*$^{-/-}$ mice. Slightly lower levels of ^{64}Cu excretion were observed in *Atp7b*$^{+/-}$ mice during the first 24 h in comparison to WT, but no differences were observed at 48 h. Regarding urinary radiocopper excretion, levels were very low and highly variable in all three groups, and no significant differences were observed among them; surprisingly, *Atp7b*$^{-/-}$ showed the lowest levels (Figure S1). Thus, radiocopper blood kinetics (BK) and fecal excretion, but not urinary excretion, represent useful biomarkers to determine copper metabolism.

Radiocopper biodistribution was analyzed by full-body *in vivo* PET, 24 and 48 h after ^{64}Cu injection. PET images in WT and *Atp7b*$^{+/-}$ animals showed the presence of radioactive signal in liver as well as in the gut region. In untreated *Atp7b*$^{-/-}$ animals, a strong signal was detected in the liver area, but no signal was detected in the gut area (Figure 2A). The quantification of the liver standardized uptake value (SUV), i.e., the radiocopper uptake in liver, showed a significantly higher hepatic retention of radiocopper in *Atp7b*$^{-/-}$ animals in comparison to WT and *Atp7b*$^{+/-}$ mice (Figure 2B). Seventy-two hours after radiocopper injection, animals were sacrificed, and the radioactive signal was quantified in liver, brain, kidneys, lungs, and spleen

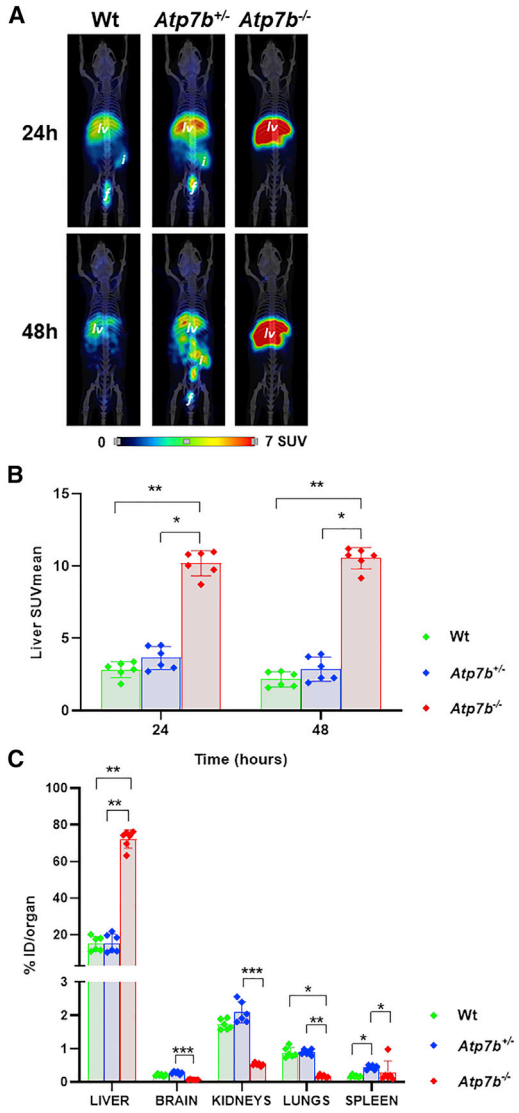

Figure 2. *In vivo* and *ex vivo* biodistribution analysis of ^{64}Cu by whole-body PET imaging and gamma counter measurements in WT, *Atp7b*$^{+/-}$, and *Atp7b*$^{-/-}$ mice at 9 weeks of age

PET analysis was performed 24 and 48 h post-^{64}Cu injection. *Ex vivo* biodistribution analysis was performed at sacrifice, 48 h after ^{64}Cu administration. (A) Representative PET coronal slices obtained 24 and 48 h after intravenous (i.v.) injection of the radiotracer co-registered with a CT 3D image of other animal used as anatomical reference. The volumes of interest (VOIs) containing the entire liver were used to obtain quantitative data. (B) Graphical representation of the quantitative measures obtained by PET data analysis is shown. (C) *Ex vivo* biodistribution data of selected organs are shown. All data were presented as mean ± SD. The statistical analysis was performed using the non-parametric Kruskal-Wallis test followed by Dunn's multiple comparison post hoc. *p < 0.05; **p < 0.01; ***p < 0.001. *lv*, liver; *i*, intestine; *f*, feces.

(Figure 2C). As observed with PET data, significantly higher radioactive signal was detected in liver of *Atp7b*$^{-/-}$ mice in comparison to livers of WT and *Atp7b*$^{+/-}$ mice. Interestingly, radiocopper levels were significantly lower in all other organs evaluated, brain, kidneys, lungs, and spleen in *Atp7b*$^{-/-}$ mice in comparison to WT or *Atp7b*$^{+/-}$ mice.

VTX-801 administration to 6-week-old Atp7b$^{-/-}$ mice significantly modifies physiological radiocopper biodistribution

Six-week-old male and female *Atp7b*$^{-/-}$ mice (n = 6) received intravenously three different doses of VTX-801: 5×10^{11}, 1.5×10^{12}, and 5×10^{12} viral genome copies (VG)/kg. The highest dose administered to animals corresponds to one previously shown to restore copper metabolism and improve survival in *Atp7b*$^{-/-}$ mice.[8] Three weeks post-injection, VTX-801-treated animals received an intravenous injection of ^{64}Cu. Blood samples were harvested at different time points, and radiocopper BK was analyzed (Figure 3A). As controls, we used untreated WT and *Atp7b*$^{-/-}$ mice from Figures 1 and 2. In *Atp7b*$^{-/-}$ animals, VTX-801 treatment prevented the continuous decrease of the radiocopper signal observed in untreated WD mice. Moreover, all three doses of VTX-801 administered showed an initial decrease in the ^{64}Cu signal followed by stabilization after 24 h. A direct dose relationship was also observed for radiocopper 48 h/1 h ratio with average values of 0.61, 0.67, and 0.79 in WD animals receiving 5×10^{11} VG/kg, 1.5×10^{12} VG/kg, and 5×10^{12} VG/kg, respectively (Figure 3B). No differences were observed depending on the gender.

Presence of radiocopper in feces also revealed a direct dose response to VTX-801 (Figures 3C and 3D), indicating that gene therapy and the expression of functional ATP7B protein restores physiological excretion of copper through the biliary and fecal route.

Radiocopper biodistribution was analyzed by PET at 24 and 48 h post [^{64}Cu]$CuCl_2$ injection. As previously described for untreated *Atp7b*$^{-/-}$ mice, copper-64 was retained in the liver and no signal was detected in the gut area; however, in animals treated with the higher dose of VTX-801, the presence of radiocopper was clearly detected in the gut region, same as in WT animals (Figure 3D). Furthermore, when ^{64}Cu activity was measured in whole organs at sacrifice (Figure 3E), a dose-dependent reduction of radiocopper activity in liver was observed for WD mice treated with VTX-801. Levels of ^{64}Cu in brain, kidneys, and lungs of untreated *Atp7b*$^{-/-}$ mice were lower than in WT animals; VTX-801 treatment at the highest dose resulted in a significant increase of ^{64}Cu in brain and lungs (Figure 3E).

Long-lasting VTX-801 restoration of fecal excretion of Cu and BK in WD mice

Six-week-old *Atp7b*$^{-/-}$ male mice (n = 3) were treated with either of four doses (5E11, 1.5E12, 5E12, and 1.5E13 VG/kg) of VTX-801 and 3 months later received an intravenous injection of [^{64}Cu]$CuCl_2$. Blood samples were harvested at different time points as previously described. The radiocopper BK of untreated WT and WD animals of matching age (18 weeks old) was different from that observed at 9 weeks of age. In WT mice, radiocopper levels remained stable from 1 to 4 h post-injection and slightly increased thereafter up to

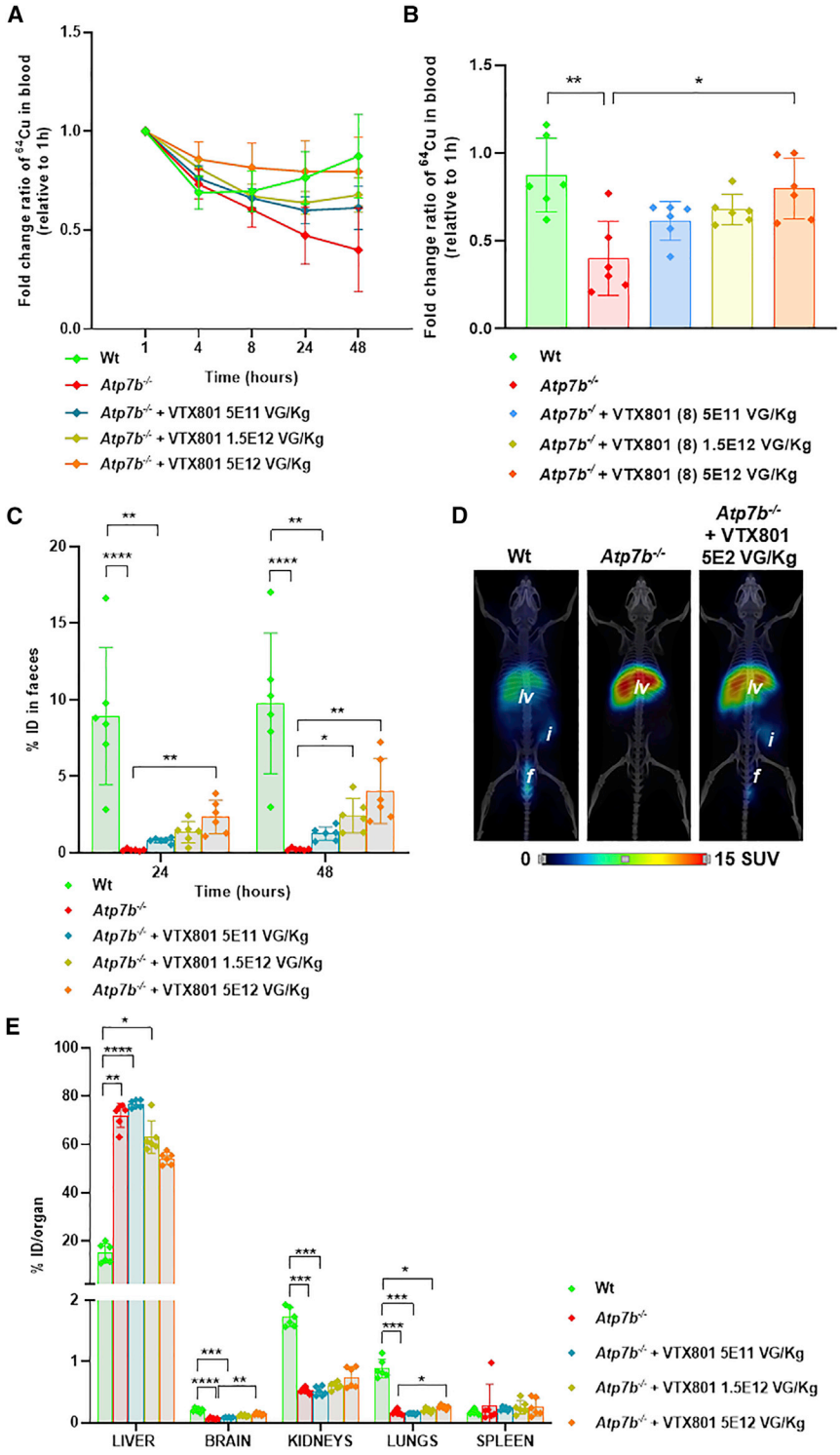

Figure 3. Copper-64 kinetics in blood and feces and *in vivo* and *ex vivo* biodistribution analysis of the radiotracer by whole-body PET imaging and gamma counter measurements in *Atp7b*$^{-/-}$, WT, and VTX-801-treated *Atp7b*$^{-/-}$ at 9 weeks of age

Atp7b$^{-/-}$ and WT mice data are the ones shown in Figures 1 and 2. Blood samples were collected 1, 4, 8, 24, and 48 h post-[^{64}Cu]$CuCl_2$ administration. Feces were harvested 24 and 48 h after ^{64}Cu injection. PET analysis was performed 24 and 48 h post-administration of the radiotracer. *Ex vivo* biodistribution analysis was performed at sacrifice, 72 h after ^{64}Cu administration. (A) Radiocopper plasma kinetics (BK), fold-change ratios of ^{64}Cu in blood at different time points relative to 1 h have been represented. (B) Forty-eight-hours-to-1-hour ratio of ^{64}Cu in the serum 1 h is shown. (C) Cumulative fecal excretion of ^{64}Cu is shown. (D) Representative PET coronal slices obtained 24 h after ^{64}Cu administration are shown. (E) *Ex vivo* biodistribution data of selected organs are shown. All data were presented as mean ± SD. The statistical analysis was performed using the non-parametric Kruskal-Wallis test followed by Dunn's multiple comparison post hoc. *p < 0.05; **p < 0.01; ***p < 0.001; ****p < 0.0001.

48 h. In WD mice, an initial drop of signal was observed during the first 8 h, followed by a sharp increase in activity levels, higher than those observed in WT animals at 48 h post-injection (Figure 4A). The average 48 h/1 h ratio of radiocopper concentration in serum was 1.32 in WT and 1.59 in WD mice (Figure 4B). Interestingly, *Atp7b*$^{-/-}$ mice treated with the two higher doses of VTX-801 (5E12 and 1.5E13 VG/kg) showed a profile similar to that observed in WT mice. At lower doses, copper-64 levels in blood either remained stable (1.5E12 VG/kg) or exhibited a continuous decrease (5E11 VG/kg) (Figure 4A), however, not as dramatic to that observed in untreated 9-week-old *Atp7b*$^{-/-}$ mice (Figure 1A). The radiocopper 48 h/1 h ratio in blood increased in a dose-dependent manner with average values of 0.6, 0.86, 1.05, and 1.06 after treatment with 5E11, 1.5E12, 5E12, and 1.5E13 VG/kg, respectively (Figure 4B).

Twenty-four-hour feces were harvested for 3 consecutive days, and the presence of radioactivity was represented as cumulative values (Figure 4C). WD animals treated with VTX-801 showed a direct dose dependency for levels of copper excreted in feces, with those that received the highest dose of VTX-801 reaching levels not significantly different from WT animals. The analysis of urinary copper-64 excretion revealed no significant differences among the different groups, although once again, levels in WT animal were slightly higher that in WD mice and WD animals treated with the highest dose of VTX-801 showed the highest levels (Figure S2).

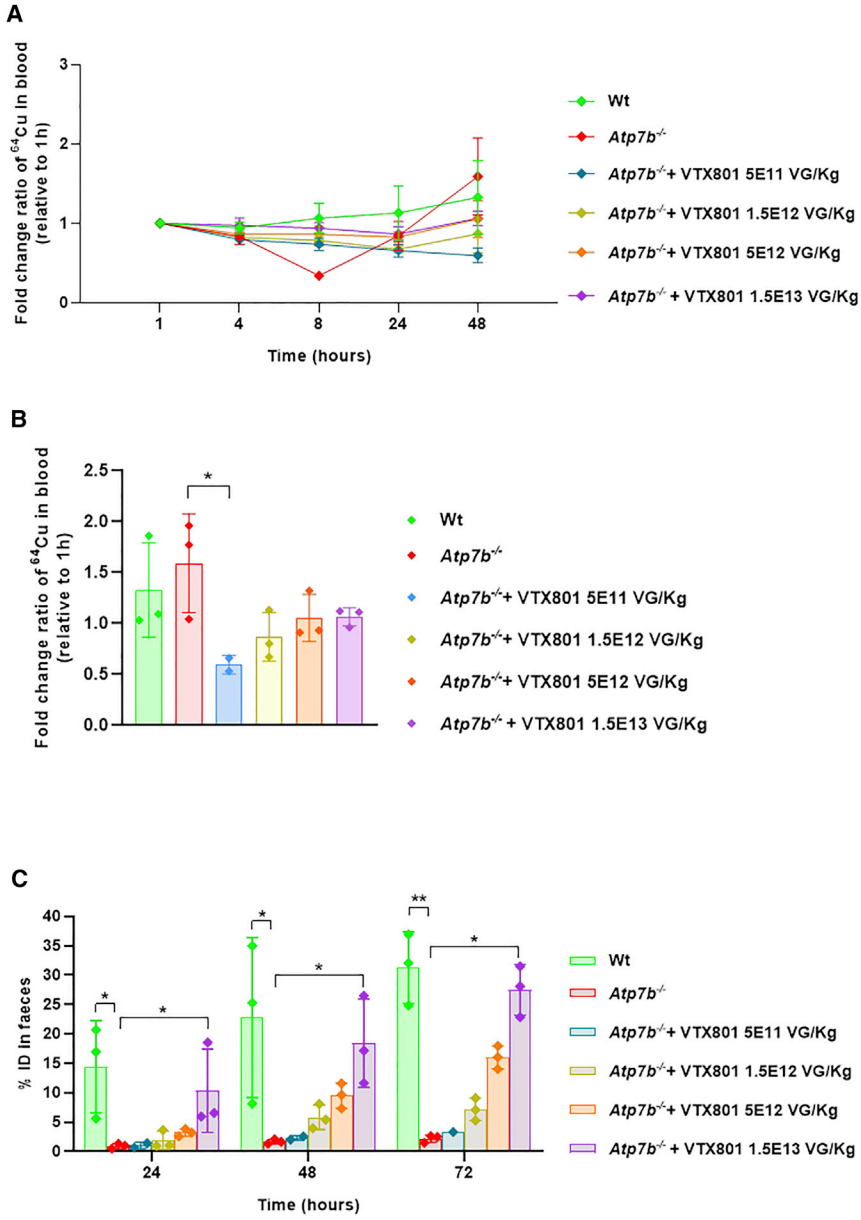

Figure 4. Copper-64 kinetics in blood and feces of *Atp7b*$^{-/-}$, WT, and VTX-801-treated *Atp7b*$^{-/-}$ mice at 18 weeks of age

Blood samples were collected 1, 4, 8, 24, 48, and 72 h post-^{64}Cu administration. Feces were harvested 24, 48, and 72 h after ^{64}Cu injection. (A) Fold change ratio of ^{64}Cu in blood relative to 1 h is shown. (B) Forty-eight-hours-to-1-hour ratio of ^{64}Cu in the serum is shown. (C) Cumulative fecal excretion of ^{64}Cu is shown. All data were presented as mean ± SD. The statistical analysis was performed using the non-parametric Kruskal-Wallis test followed by Dunn's multiple comparison post hoc. *$p < 0.05$; **$p < 0.01$.

PET images revealed retention of radiocopper in liver of untreated *Atp7b*$^{-/-}$ mice. VTX-801 treatment induced a dose-dependent reduction of ^{64}Cu signal in the liver area as well as a dose-dependent increase of radiocopper signal in the gut area (Figure 5A). Furthermore, radiocopper signal was also quantified by drawing volumes of interest (VOIs) in liver at 90 min (min), 24 h, and 48 h after ^{64}Cu injection and 24 h/90 min or 48 h/90 min ratios were calculated (Figure 5B). In WT animals, both ratios were below 1, indicating a reduction of radiocopper in liver over time. In contrast, untreated *Atp7b*$^{-/-}$ mice exhibited ratios above 1, suggesting retention of the radiotracer in the organ. WD mice treated with VTX-801 showed a dose-dependent reduction of ^{64}Cu signal in liver as well as a reduction in the 24 h/90 min or 48 h/90 min ratios in comparison to WD untreated mice.

At sacrifice, radioactive signal was quantified in liver, brain, kidneys, lungs, and spleen. A VTX-801 dose-dependent reduction in hepatic ^{64}Cu concentration was observed (Figure 5C). The radioactive signal was increased in kidneys and lungs at higher doses of vector at similar levels to WT (no significant differences). Interestingly, high levels of radiocopper were found in the spleen of 18-week-old untreated *Atp7b*$^{-/-}$ animals (not observed in 9-week-old animal) that were significantly reduced by VTX-801 treatment (Figure 5C).

DISCUSSION

The *Atp7b* knockout (*Atp7b*$^{-/-}$) mouse is a good model of WD, allowing proof-of-concept and pharmacology studies of AAV-mediated gene therapy. It exhibits the typical biochemical and pathophysiological alterations found in WD patients, including progressive liver involvement and lack of biliary elimination of copper. The advantages of the *Atp7b*$^{-/-}$ mouse model to test the therapeutic efficacy of gene therapy approaches include a well-defined genetic background, good survival with disease progression, good AAV-transduction efficiency, and availability of the original strain to serve as a control in comparative analyses.[15] We demonstrated that an AAV vector carrying an *ATP7B*-minigene (named VTX-801) was able to restore copper metabolism and physiological copper excretion in WD mice in a safe and very efficient manner.[8] Next, and in anticipation of a future clinical study, we worked on the development of a clinically compatible and minimally invasive method to demonstrate the efficacy of gene therapy in restoring copper metabolism in WD patients.

Copper-64 is a radionuclide that exhibits physical properties that are complementary for diagnosis, therapeutic purposes, and

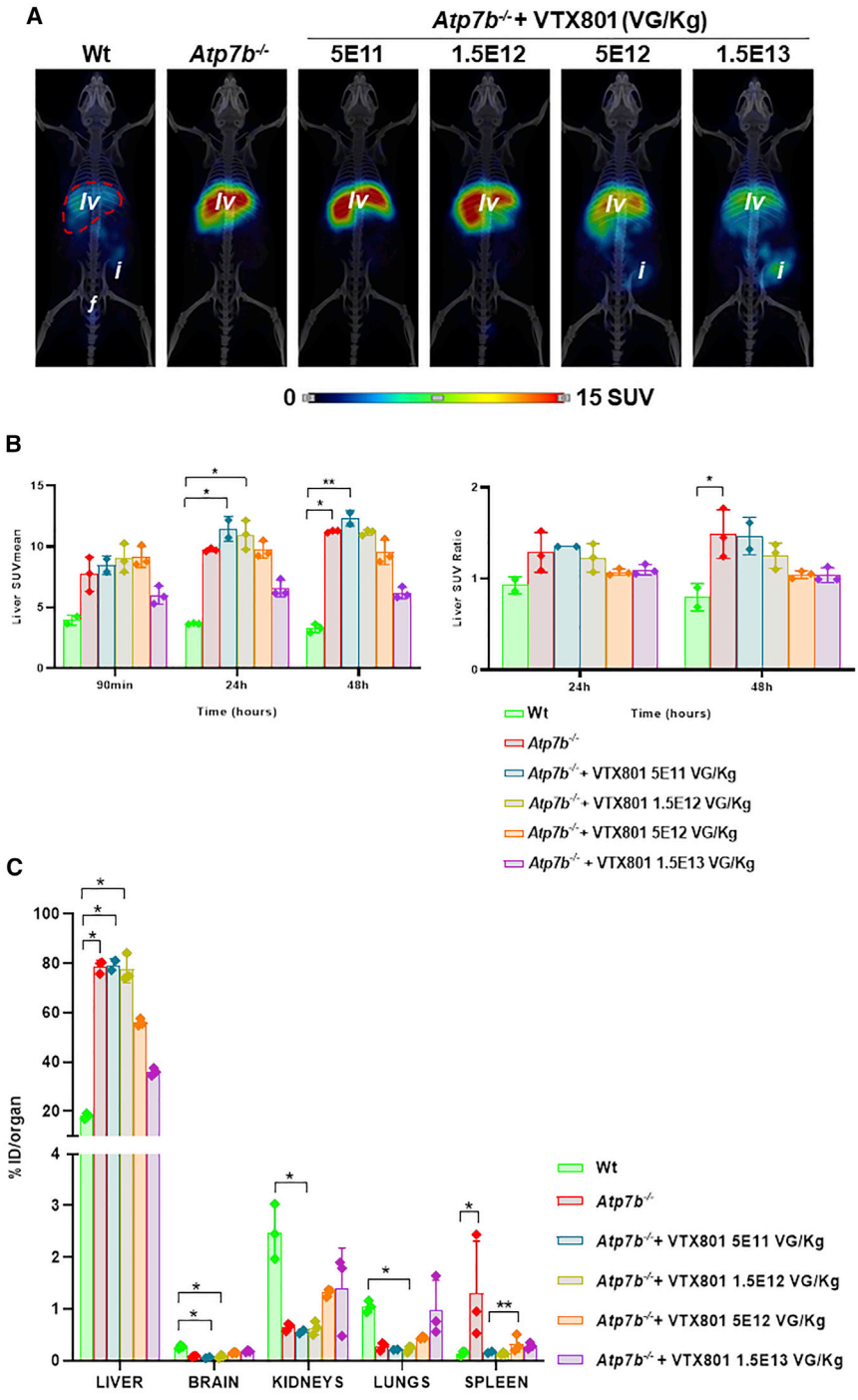

Figure 5. *In vivo* and *ex vivo* biodistribution analysis of ^{64}Cu by whole-body PET imaging and gamma counter measurements in *Atp7b*$^{-/-}$, WT, and VTX-801-treated *Atp7b*$^{-/-}$ mice at 18 weeks of age

PET analysis was performed 90 min and 24 and 48 h post-^{64}Cu injection. *Ex vivo* biodistribution analysis was performed at sacrifice, 72 h after ^{64}Cu administration. (A) Representative PET coronal slices obtained 48 h after the injection of the radiotracer are shown. The VOIs)containing the entire liver (dashed line) were used to obtain quantitative data. (B) Graphical representation of hepatic concentration of ^{64}Cu (SUV) at 90 min and 24 and 48 h post-injection and ratio of 24 h/90 min and 48 h/90 min hepatic SUV values derived from PET data analysis is shown. (C) *Ex vivo* biodistribution data of selected organs are shown. All data were presented as mean ± SD. The statistical analysis was performed using the non-parametric Kruskal-Wallis test followed by Dunn's multiple comparison post hoc. *p < 0.05; **p < 0.01.

biodistribution studies. In different types of cancers, copper-64 is being used both as a theranostic agent and to monitor the efficacy of antitumoral agents.[16,17] Furthermore, copper-64 labeling of antibodies, small molecules, nanoparticles, or cells followed by PET imaging represent a highly sensitive and non-invasive method for biodistribution and pharmacokinetic studies.[18–20] Although clinical experience is still relatively limited, so far, no adverse effects have been described associated with the use of copper-64 at the doses administered.

Starting from the 50s–60s, copper-64 has been used to explore the copper metabolism in healthy volunteers and WD patients, as a diagnostic tool for WD and as a highly sensitive technique to determine copper uptake by the liver, fecal copper excretion, and incorporation of copper into ceruloplasmin.[10–13] In animal models, the use of copper-64 biodistribution analysis has been shown to differentiate between WD and WT animals.[21–23] Interestingly, Sternlieb and Scheinberg[13] used the 48 h/1 h or 48 h/2 h ^{64}Cu ratio of radiocopper signal in the serum as an index of copper incorporation into ceruloplasmin that distinguishes homozygote from heterozygote *ATP7B* mutation carriers. This parameter has been recently used by Członkowska et al.,[14] confirming the excellent diagnostic accuracy of the 48 h/2 h copper-64 ratio. In our study, we found that the parameter used by Sternlieb (48 h/1 h radiocopper ratio in blood) allowed us to distinguish WT from WD animals at 9 weeks of age. But more importantly, the administration of VTX-801 normalized this ratio in WD mice in a dose-dependent manner. However, at 18 weeks of age, we observed a very different pattern; while 9-week-old WD mice presented a progressive reduction of radiocopper in blood, 18-week-old WD animals showed, after an initial decay, a sharp increase of ^{64}Cu activity in blood, reaching at 24 h and 48 h levels that were even higher than those of age-matched WT animals. In WT animals, the increase of radiocopper in circulation is due to the

ATP7B-mediated radiocopper loading into ceruloplasmin. In WD, due to the absence of ATP7B, this should not be possible; however, we have previously shown that, in WD animals, ceruloplasmin activity spontaneously increases with disease progression and development of liver damage.[7] In fact, we further demonstrated that the induction of liver injury in WD mice by the administration of an adenovirus resulted in an increase in ceruloplasmin activity in circulation. Thus, in 18-week-old WD mice, ceruloplasmin is acting as an acute phase reactant, as has been also shown in WD patients during acute liver injury.[24] Interestingly, VTX-801 administration changed significantly copper-64 blood BK in 18-week-old WD mice. Even at the lowest dose of VTX-801, which has a very minor effect over the reduction of hepatic copper-64 retention, we observed a significant change in the radiocopper BK in comparison to untreated WD mice, which is more similar to the one shown by asymptomatic untreated 9-week-old WD mice. This observation could be explained by the fact that very low doses of VTX-801 are capable of controlling liver damage in WD mice but are not enough to increase the levels of ceruloplasmin in circulation.[7,8] Importantly, the administration of higher VTX-801 doses normalized copper-64 48 h/1 h ratios in a dose-dependent manner in blood. Thus, the analysis of copper-64 BK in conjunction to acute injury biomarkers to discard spontaneous ceruloplasmin secretion might represent a reliable biomarker to determine the effect of VTX-801 over the restoration of ceruloplasmin levels in blood. Furthermore, in our study, we observed that, due to the absence of ATP7B, WD mice retained close to 80% of the radiocopper injected in the liver and showed a clear impairment for biliary copper excretion as determined by PET imaging and analysis of radiocopper in feces. Similar results were obtained in patients and WD animal models.[21–23,25–27] In WT animals, excess of copper is excreted via the biliary and fecal route, while in WD mice, copper is accumulated in the liver and eliminated through the urine; however, this is insufficient to restore an appropriate balance with dietary intake, as toxic copper levels accumulate in tissues, primarily in the liver. VTX-801 administration significantly reduced hepatic copper-64 retention and increased biliary and fecal excretion in a dose-dependent manner at 9 and 18 weeks of age. At the higher dose of VTX-801, most parameters associated with copper metabolism and excretion were very similar to WT animals. Interestingly, in *Atp7b*$^{-/-}$ mice, copper is mainly excreted throughout the urine, showing significantly higher levels than WT animals. Shortly after VTX-801 administration, we observed a highly efficient reduction in Cu concentration in urine, even at the lowest dose of vector. However, the analysis of copper-64 concentration in the urine of WD and WT animals revealed no significant differences but a tendency to lower levels in WD animals than in WT, which is contrary to what we were expecting and can be explained by the strong radiocopper retention in liver of WD animals.

Recently, Sandahl et al.[28] showed that, using a simple 20-h-to-90-min mean SUV ratio of the liver, copper-64 PET and computed tomography (CT) diagnosed WD patients with 100% accuracy. Here, we have used this ratio to estimate the effect of VTX-801 treatment over copper-64 liver retention in *Atp7B*$^{-/-}$ mice (Figure 5B). At 48 h, the SUV ratio value was below 1 in WT animals and above 1 in WD mice, indicating that copper-64 was being removed from the liver in WT animals and was retained and accumulated in WD mice liver. VTX-801 reduced this ratio in a dose-dependent manner. These results are in agreement with Sandahl et al.[28] observations and suggest that this parameter, apart from being of high value for WD diagnosis, is also an attractive tool to evaluate the pharmacodynamics of a gene-therapy product aiming at the restoration of physiological copper metabolism. However, it should be noted that Sandahl's study,[28] contrary to our work or that of Osborn and Walshe,[11] showed that, at early time points (i.e., 90 min after ^{64}CuCl2 injection), hepatic copper-64 uptake was lower in WD patients than in healthy and heterozygotes subjects. The difference between the studies of Sandahl et al. and Osborn and Walshe could be due to the different characteristics of the patients with WD included. Although limited information is available, most likely in the recent study by Sandahl et al., the patients are being controlled by copper chelation or Zn salts, while in Osborn and Walshe, the patients remain untreated like our control WD mice.

Regarding copper-64 biodistribution, we observed lower levels in the brain, kidneys, and lungs of WD mice than of WT animals, both at 9 and 18 weeks of age. As suggested before to explain the unexpected results obtained in the urine, this could be related to the retention of the copper-64 in the liver. Interestingly, after VTX-801 treatment, we observed a tendency to increase the copper-64 levels in those organs in a dose-dependent manner. In the case of the brain, a relevant organ in WD due to the neurological aspects of the disease, our results correlated with those reported by Peng et al.[22] and Xie et al.,[29] showing lower levels of radiocopper in the brain of WD in young animals in comparison to WT animals. However, Xie et al. showed that this pattern changed in older animals that showed more radiocopper in the brain of WD mice than in WT animals.[29] Experiments in older animals will be of interest to determine whether VTX-801 prevents radiocopper accumulation in the brain of WD animals.

An observation that is of interest but that also required additional experimentation to understand the mechanism is the high levels of radiocopper observed in the spleen of *Atp7b*$^{-/-}$ at 18 weeks of age, but not at 9 weeks. Those levels were reduced in VTX-801-treated mice, even at the lowest dose of vector, correlating with the presence of lower copper-64 in the blood circulation.

Currently available treatments for WD patients are based on daily administration of copper chelators (D-penicillamine and trientine) or zinc salts. Copper chelators work by inducing urinary copper excretion, while zinc salts act mainly by inhibiting intestinal copper absorption.[5] As opposed to VTX-801, none of these medical treatments restore fecal copper-64 elimination and holo-ceruloplasmin production. Therefore, the use of radiocopper might provide a unique opportunity to differentiate the pharmacodynamic effects of VTX-801 in patients under chelator or Zn treatment.

MATERIALS AND METHODS

Animals and radiopharmaceuticals

All animal procedures were performed according to an ethic protocol specifically drafted for this project. The protocol was evaluated and approved by the University of Navarra's Ethics Committee for Animal Experimentation (protocol code number: CEEA/019-18) and further approved by the Department of Health of the Navarra Government on 13/03/2018. WD animal model *Atp7b*$^{-/-}$ and heterozygous mice *Atp7b*$^{+/-}$ were generated at CIMA by backcrossing *Atp7b*$^{-/-}$ C57BL/6 × 129S6/SvEv (*15*) obtained from Jackson Laboratories with WT C57BL/6 purchased from Janvier. Mice were socially housed in ventilated cages in an air-conditioned room at 22°C under a 12 h light/dark cycle with access to food and tap water *ad libitum*.

Mice (n = 3–6) were injected with [^{64}Cu]$CuCl_2$ intravenously via the tail vein (final volume: 100 μL; dose: 12.1 ± 2.1 MBq). [^{64}Cu]$CuCl_2$ was purchased from CIC biomaGUNE (San Sebastián, Spain), and it was produced via ^{64}Ni(p,n)^{64}Cu nuclear reaction on an IBA Cyclone 18/9 cyclotron and immediately purified to obtain [^{64}Cu]$CuCl_2$ in a 0.1 M HCl solution. The specific activity of the radiotracer was 40 ± 16 GBq/μmol. During the experimental procedure, mice were housed individually in metabolic cages separated by gender.

VTX-801 production

The recombinant AAV (rAAV) genome carrying a therapeutic expression cassette containing a shortened version of the human *ATP7B* gene (*ATP7B*-minigene) under the transcriptional control of the liver-specific α1-antitrypsin promoter (AATp) has been described previously.[8] The main characteristics of the vector preparation are shown in Figure S3. For virus titration, viral DNA was isolated using the High Pure Viral Nucleic Acid kit (Roche Applied Science. Mannheim, Germany). Viral titer, measured as VG/mL, was determined by qPCR (Applied Biosystems, Foster City, CA) using the following primers: AATp forward primer 5′-TTGCTCCTC CGATAACTGGG-3′ and AATp reverse primer 5′-CCCTGTCCTC GTCCGTATTT-3′.

Biological sampling

After [^{64}Cu]$CuCl_2$ injection, several biological samples were collected and radioactivity (Bq) was counted on a gamma counter (Hidex Automatic Gamma Counter). Blood samples were collected and weighted. The % injected dose (ID)/g of blood was calculated considering the decay of copper-64, and data were represented in the graph as the fold change ratio relative to 1 h. Urine and feces were harvested throughout 24 h from individual animals using metabolic cages, and data were expressed as the % ID correcting the radioactive decay of copper-64.

In vivo PET imaging and *ex vivo* copper-64 biodistribution

All PET scans were obtained in a dedicated small-animal imaging tomograph (Mosaic, Philips), with an axial and transaxial field of view of 11.9 and 12.8 cm, respectively, and a full width at half maximum resolution of 2.1 mm. At 1.5, 24 and 48 h post-injection, mice were placed prone on the PET scanner under continuous anesthesia with isoflurane (2% in 100% O_2 gas) to acquire a static image (sinogram) within 15 min. All the images were reconstructed in a 128 × 128 matrix with a 1 × 1 × 1 mm^3 voxel size using the 3D Ramla algorithm with two iterations and a relaxation parameter of 0.024. Dead time, decay, random, and scattering corrections were applied during the reconstruction process. All the studies were exported and analyzed using the PMOD software (PMOD Technologies, Adliswil, Switzerland). Images were expressed in SUV units, using the formula $SUV = \left[\frac{tissue\ activity\ concentration(Bq/cm^3)}{injected\ dose\ (Bq)}\right] \times body\ weight(g)$. A spherical VOI containing the entire liver was drawn over PET images to obtain semi-quantitative data. Then, a semiautomatic delineation tool was used (applying a predefined threshold of 40% of the maximum voxel value) to obtain a new VOI that delimited the liver with copper-64 uptake. Finally, SUVmean, which was defined as the average SUV of voxels within the VOI, was calculated. To determine the kinetics of copper-64 elimination from the liver, we calculated the ratio between the liver mean SUV values obtained at 24 and 48 h and those obtained at 90 min.

For *ex vivo* analysis 72 h post-^{64}Cu administration, liver, brain, kidneys, lungs, and spleen were dissected as a whole at sacrifice. All tissues were weighed and subjected to radioactivity (Bq) measurement with a gamma counter (Hidex Automatic Gamma Counter). Copper-64 biodistribution was expressed as % of ID per organ, correcting the measurement with the calculated radioactive decay at any given time point.

Properly calibrated radioactivity measurement systems were used. Particularly, daily stability measurements are done both for the microPET and the gamma counter, and the accuracy of both systems is routinely verified on a monthly basis to ensure that quantitative values deviate less than 10% from the true value.

Statistical analysis

Data are presented as mean values ± standard deviation and were analyzed for significance by the non-parametric Kruskal-Wallis test followed by the Dunn's multiple comparison post hoc using GraphPad Prism 8.00 software (GraphPad Software, CA, USA).

SUPPLEMENTAL INFORMATION

Supplemental information can be found online at https://doi.org/10.1016/j.omtm.2022.06.001.

ACKNOWLEDGMENTS

Infrastructure and technical support were provided by the animal facility staff at CIMA. The authors thank Xiao Ru and Luk Vandenberghe for advice and support on AAVAnc80 production. This work was supported by Vivet Therapeutics.

AUTHOR CONTRIBUTIONS

Study concept and design, O.M., M.C., I.P., B.B., and G.G.-A.; acquisition of data, O.M., D.M., C.G., M.B., M.E., and B.T.; analysis and

interpretation of data and drafting of the manuscript, O.M., D.M., C.G., B.T., R.H.-A., V.F., A.D., B.B., J.P.C., and G.G.-A.; critical revision of the manuscript for important intellectual content, A.D., V.F., and J.P.C.; statistical analysis, O.M., M.C., V.F., B.B., and G.G.-A.; obtained funding, A.D., G.G.-A., and J.P.C.; study supervision, B.T., V.F., A.D., I.P., B.B., and G.G.-A.

DECLARATION OF INTERESTS

O.M., R.H.-A., and G.G.-A. are co-inventors of VTX-801; B.T., A.D., V.F., B.B., J.P.C., and G.G.-A. are Vivet Therapeutics SAS employees—B.B., J.P.C., and G.G.-A. hold stock, and J.P.C. and G.G.-A. are founders of the company. The other authors declare no competing interests.

REFERENCES

1. Członkowska, A., Litwin, T., Dusek, P., Ferenci, P., Lutsenko, S., Medici, V., Rybakowski, J.K., Weiss, K.H., and Schilsky, M.L. (2018). Wilson disease. Nat. Rev. Dis. Primers *4*, 21. https://doi.org/10.1038/s41572-018-0018-3.
2. Saroli Palumbo, C., and Schilsky, M.L. (2019). Clinical practice guidelines in Wilson disease. Ann. Transl. Med. *7*, S65. https://doi.org/10.21037/atm.2018.12.53.
3. Ferenci, P. (2017). Diagnosis of Wilson disease. Handb. Clin. Neurol. *142*, 171–180. https://doi.org/10.1016/B978-0-444-63625-6.00014-8.
4. European Association for Study of Liver (2012). EASL clinical practice guidelines: wilson's disease. J. Hepatol. *56*, 671–685. https://doi.org/10.1016/j.jhep.2011.11.007.
5. Roberts, E.A., and Schilsky, M.L.; American Association for Study of Liver Diseases (AASLD) (2008). Diagnosis and treatment of Wilson disease: an update. Hepatology *47*, 2089–2111. https://doi.org/10.1002/hep.22261.
6. Poujois, A., Sobesky, R., Meissner, W.G., Brunet, A.S., Broussolle, E., Laurencin, C., Lion-François, L., Guillaud, O., Lachaux, A., Maillot, F., et al. (2020). Liver transplantation as a rescue therapy for severe neurologic forms of Wilson disease. Neurology *94*, e2189–e2202. https://doi.org/10.1212/WNL.0000000000009474.
7. Murillo, O., Luqui, D.M., Gazquez, C., Martinez-Espartosa, D., Navarro-Blasco, I., Monreal, J.I., Guembe, L., Moreno-Cermeño, A., Corrales, F.J., Prieto, J., et al. (2016). Long-term metabolic correction of Wilson's disease in a murine model by gene therapy. J. Hepatol. *64*, 419–426. https://doi.org/10.1016/j.jhep.2015.09.014.
8. Murillo, O., Moreno, D., Gazquez, C., Barberia, M., Cenzano, I., Navarro, I., Uriarte, I., Sebastian, V., Arruebo, M., Ferrer, V., et al. (2019). Liver expression of a MiniATP7B gene results in long-term restoration of copper homeostasis in a Wilson disease model in mice. Hepatology *70*, 108–126. https://doi.org/10.1002/hep.30535.
9. Moreno, D., Murillo, O., Gazquez, C., Hernandez-Alcoceba, R., Uerlings, R., Gonzalez-Aseguinolaza, G., and Weiskirchen, R. (2018). Visualization of the therapeutic efficacy of a gene correction approach in Wilson's disease by laser-ablation inductively coupled mass spectrometry. J. Hepatol. *68*, 1088–1090. https://doi.org/10.1016/j.jhep.2017.12.022.
10. Bearn, A.G., and Kunkel, H.G. (1954). Localization of Cu64 in serum fractions following oral administration: an alteration in Wilson's disease. Proc. Soc. Exp. Biol. Med. *85*, 44–48. https://doi.org/10.3181/00379727-85-20780.
11. Osborn, S.B., and Walshe, J.M. (1967). Studies with radioactive copper (64Cu and 67Cu) in relation to the natural history of Wilson's disease. Lancet *1*, 346–350. https://doi.org/10.1016/s0140-6736(67)92893-0.
12. O'Reilly, S., Weber, P., Pollycove, M., and Shipley, L. (1969). Detection of the heterozygote of Wilson's disease. J. Nucl. Med. *10*, 143–144.
13. Sternlieb, I., and Scheinberg, I.H. (1972). Radiocopper in diagnosing liver disease. Semin Nucl. Med. *2*, 176–188. https://doi.org/10.1016/s0001-2998(72)80071-0.
14. Członkowska, A., Rodo, M., Wierzchowska-Ciok, A., Smolinski, L., and Litwin, T. (2018). Accuracy of the radioactive copper incorporation test in the diagnosis of Wilson disease. Liver Int. *38*, 1860–1866. https://doi.org/10.1111/liv.13715.
15. Buiakova, O.I., Xu, J., Lutsenko, S., Zeitlin, S., Das, K., Das, S., Ross, B.M., Mekios, C., Scheinberg, I.H., and Gilliam, T.C. (1999). Null mutation of the murine ATP7B (Wilson disease) gene results in intracellular copper accumulation and late-onset hepatic nodular transformation. Hum. Mol. Genet. *8*, 1665–1671. https://doi.org/10.1093/hmg/8.9.1665.
16. Keinänen, O., Fung, K., Brennan, J.M., Zia, N., Harris, M., van Dam, E., Biggin, C., Hedt, A., Stoner, J., Donnelly, P.S., et al. (2020). Harnessing ^{64}Cu/^{67}Cu for a theranostic approach to pretargeted radioimmunotherapy. Proc. Natl. Acad. Sci. USA *117*, 28316–28327. https://doi.org/10.1073/pnas.2009960117.
17. Mirzaei, S., Mohammed, F., and Zandieh, S. (2020). Theranostics of metastatic prostate cancer applying 64Cu/18F/68Ga PSMA PET-CT and 177Lu radiopharmaceuticals. Curr Radiopharm. https://doi.org/10.2174/1874471013666200908122845.
18. Krishnan, A., Adhikarla, V., Poku, E.K., Palmer, J., Chaudhry, A., Biglang-Awa, V.E., Bowles, N., Nathwani, N., Rosenzweig, M., Sahebi, F., et al. (2020). Identifying CD38+ cells in patients with multiple myeloma: first-in-human imaging using copper-64-labeled daratumumab. Blood Adv. *4*, 5194–5202. https://doi.org/10.1182/bloodadvances.2020002603.
19. Caserta, E., Chea, J., Minnix, M., Poku, E.K., Viola, D., Vonderfecht, S., Yazaki, P., Crow, D., Khalife, J., Sanchez, J.F., et al. (2018). Copper 64-labeled daratumumab as a PET/CT imaging tracer for multiple myeloma. Blood *131*, 741–745. https://doi.org/10.1182/blood-2017-09-807263.
20. Mortimer, J.E., Bading, J.R., Park, J.M., Frankel, P.H., Carroll, M.I., Tran, T.T., Poku, E.K., Rockne, R.C., Raubitschek, A.A., Shively, J.E., et al. (2018). Tumor uptake of ^{64}Cu-DOTA-Trastuzumab in patients with metastatic breast cancer. J Nucl. Med. Jan *59*, 38–43. https://doi.org/10.2967/jnumed.117.193888.
21. Yezdimer, E.M., Umemoto, T., Yamada, H., Makino, S., and Tooyama, I. (2013). Visualizing hepatic copper release in Long-Evans cinnamon rats using single-photon emission computed tomography. Appl. Biochem. Biotechnol. *170*, 1138–1150. https://doi.org/10.1007/s12010-013-0252-9.
22. Peng, F., Lutsenko, S., Sun, X., and Muzik, O. (2012). Positron emission tomography of copper metabolism in the Atp7b-/- knock-out mouse model of Wilson's disease. Mol. Imaging Biol. *14*, 70–78. https://doi.org/10.1007/s11307-011-0476-4.
23. Peng, F., Lutsenko, S., Sun, X., and Muzik, O. (2012). Imaging copper metabolism imbalance in Atp7b (-/-) knockout mouse model of Wilson's disease with PET-CT and orally administered 64CuCl2. Mol. Imaging Biol. *14*, 600–607. https://doi.org/10.1007/s11307-011-0532-0.
24. Eisenbach, C., Sieg, O., Stremmel, W., Encke, J., and Merle, U. (2007). Diagnostic criteria for acute liver failure due to Wilson disease. World J Gastroenterol. *13*, 1711–1714. https://doi.org/10.3748/wjg.v13.i11.1711.
25. Kjærgaard, K., Sandahl, T.D., Frisch, K., Vase, K.H., Keiding, S., Vilstrup, H., Ott, P., Gormsen, L.C., and Munk, O.L. (2020). Intravenous and oral copper kinetics, biodistribution and dosimetry in healthy humans studied by 64copper PET/CT. EJNMMI Radiopharm Chem *5*, 15. https://doi.org/10.1186/s41181-020-00100-1.
26. Pfeiffer, R.F. (2020). Diagnosing wilson's disease under the sword of damocles. Neurol. Neurochir. Pol. *54*, 364–365. https://doi.org/10.5603/PJNNS.2020.0086.
27. Bahde, R., Kapoor, S., Bhargava, K.K., Schilsky, M.L., Palestro, C.J., and Gupta, S. (2012). PET with Cu-histidine for noninvasive diagnosis of biliary copper excretion in Long- Evans cinnamon rat model of Wilson disease. J. Nucl. Med. *53*, 961–968. https://doi.org/10.2967/jnumed.111.092361.
28. Sandahl, T.D., Gormsen, L.C., Munk, O.L., Kjærgaard, K., Bender, D., Vase, K.H., Frisch, K., Von Arenstorff Vilstrup, H., Keiding, S., and Ott, P. (2019). Evaluation of human copper metabolism and diagnosis of Wilson disease by ^{64}CuCl2 positron emission tomography. Hepatology *70*, 1–187. https://doi.org/10.1002/hep.30940.
29. Xie, F., Xi, Y., Pascual, J.M., Muzik, O., and Peng, F. (2017). Age-dependent changes of cerebral copper metabolism in Atp7b$^{-/-}$ knockout mouse model of Wilson's disease by [64Cu]CuCl2-PET/CT. Metab. Brain Dis. *32*, 717–726. https://doi.org/10.1007/s11011-017-9956-9.